Zeitschrift: Schweizerische mineralogische und petrographische Mitteilungen = Bulletin suisse de minéralogie et pétrographie

Band: 57 (1977)

Heft: 3

Artikel: The manganese deposits of Buritirama (Pará, Brazil)

Autor: Peters, Tj. / Valarelli, J.V. / Coutinho, J.M.V.

DOI: https://doi.org/10.5169/seals-44438

Schweiz. mineral. petrogr. Mitt. 57, 313–327, 1977

The Manganese Deposits of Buritirama (Pará, Brazil)

By *Tj. Peters*[1]), *J. V. Valarelli*[2]), *J. M. V. Coutinho*[2]), *J. Sommerauer*[3]) and *J. von Raumer*[4])

Abstract

In the Serra do Buritirama numerous lensoid bodies of supergene manganese ore, composed of cryptomelane, lithiophorite, nsutite and busetite occur. The unaltered protore consists of manganese calc-silicate marbles with small pods of braunite. The carbonates, pyroxenoids, garnets, tephroite, braunite, manganophyllite and sulfides of the protores and associated rocks were studied in detail optically, by X-ray and microprobe to evaluate the physical chemical conditions of the metamorphism in amphibolite facies that affected the region. Low variance mineral assemblages suggest temperatures of metamorphism around 500–550°C, and oxygen fugacities higher than 10^{-10} bar. Fluid inclusions infer corresponding pressures of about 3 kbar, at high X_{CO_2}.

It is concluded that the ore was deposited as a manganiferous limestone dolomite sequence in a shallow platform basin from terrestrial weathering products.

Introduction and geological aspects

The manganese deposits of Serra de Buritirama as well as the huge iron deposits of the Serra dos Carajás are situated in the central-east part of Para State in the region drained by the Itacaiunas river, between the 5° 30′ to 6° 30′ S latitude and 50′ W Greenwich (Fig. 1).

The vast Pre-cambrian terrain is part of the Guaporé Craton. The oldest polymetamorphic gneissic and amphibolitic rocks are locally named Xingu Complex, and the overlying metasedimentary sequence belongs to the Grão Pará Group.

In the Serra dos Carajás region, 100 km south of Buritirama, the rocks of the Grão Pará are predominantly schists, quartzites and two basic metavolcanic sequences containing the Iron Formation (Itabirites; TOLBERT et al., 1971).

[1]) Min. Petr. Institute, University of Bern, Sahlistrasse 6, CH-3012 Berne.
[2]) Instituto de Geociências, Universidade de São Paulo, Brasil.
[3]) Inst. f. Kristallographie und Petrographie, ETH-Zentrum, CH-8092 Zürich.
[4]) Mineralog. Institut, Université, CH-1700 Fribourg.

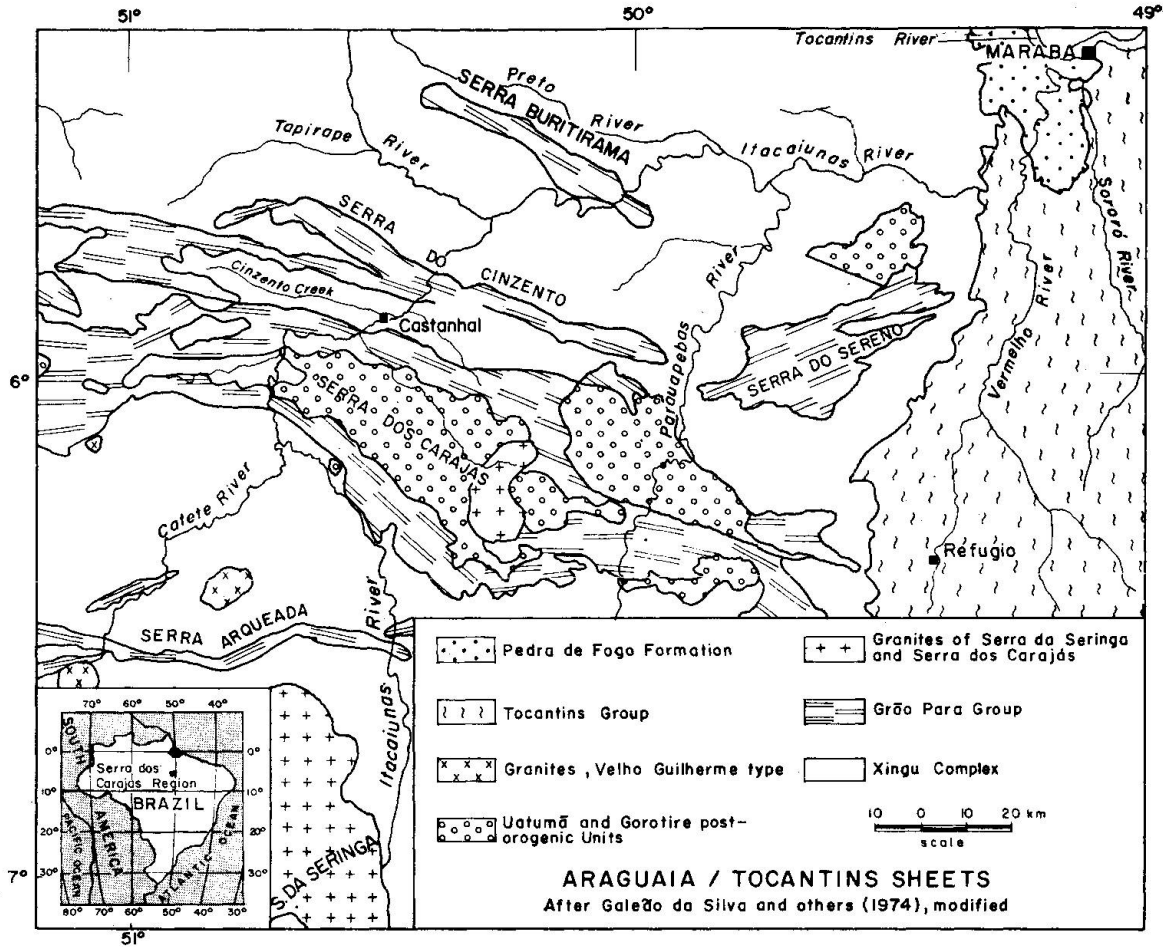

Fig. 1. Localization map and regional geology of the Serra dos Carajás region, including the Serra de Buritirama area (modified after GALEÃO DA SILVA and others, 1974; as in GOMES and others, 1975).

Overlying the Grão Pará Group discordantly, there is a sequence of molassic sediments represented by conglomeratic sandstones, siltites, shales and marbles – the Uatuma Group – correlated to the Rio Fresco Formation. This sequence contains manganese deposits similar to those from Francevillien Series of Gabon (WEBER and VALARELLI, in preparation).

Many little lensoid manganese bodies averaging 180 m in length are found in the area (Fig. 2). By way of exception B_4 presents three mineralized areas totaling 3.3 km in length.

The best known B_5 orebody is 1,400 m long, 35–240 m wide and 5–30 m thick. A cross section (Fig. 3) shows weathered protores (manganese calc-silicate marbles and schists) interbedded with mica schists placed beneath sugary quartzite and above sericite quartzites all in a same general attitude of N-60-W, 20–30° NE.

The massive, hard, concretionary, high-Mn ore (46–47%) is restricted to the first 1–3 meters, grading rapidly downwards to a finegrained mixture of

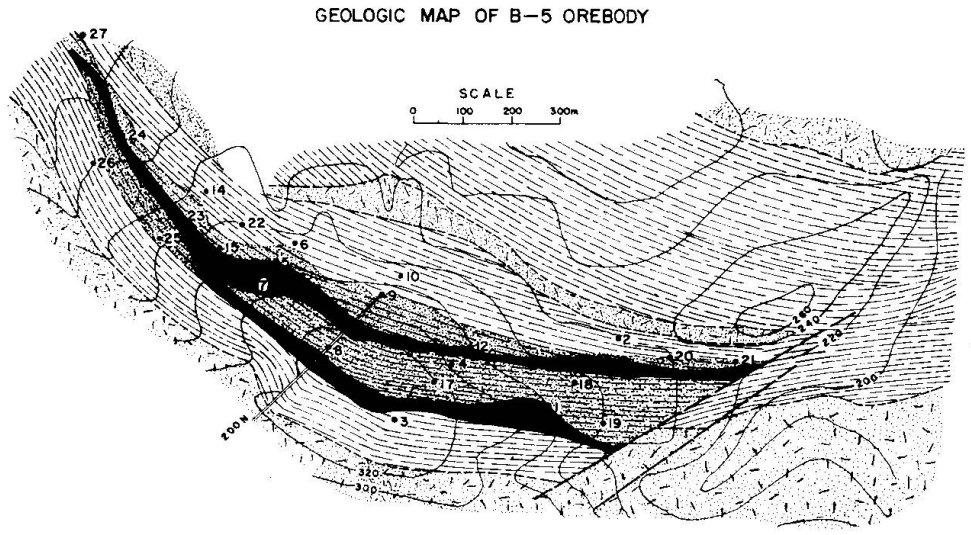

Fig. 2. Geology of the Buritirama (B-5) orebody after ANDERSON, DYER and TORRES (1974) (simplified). Legend is the same as in Fig. 3.

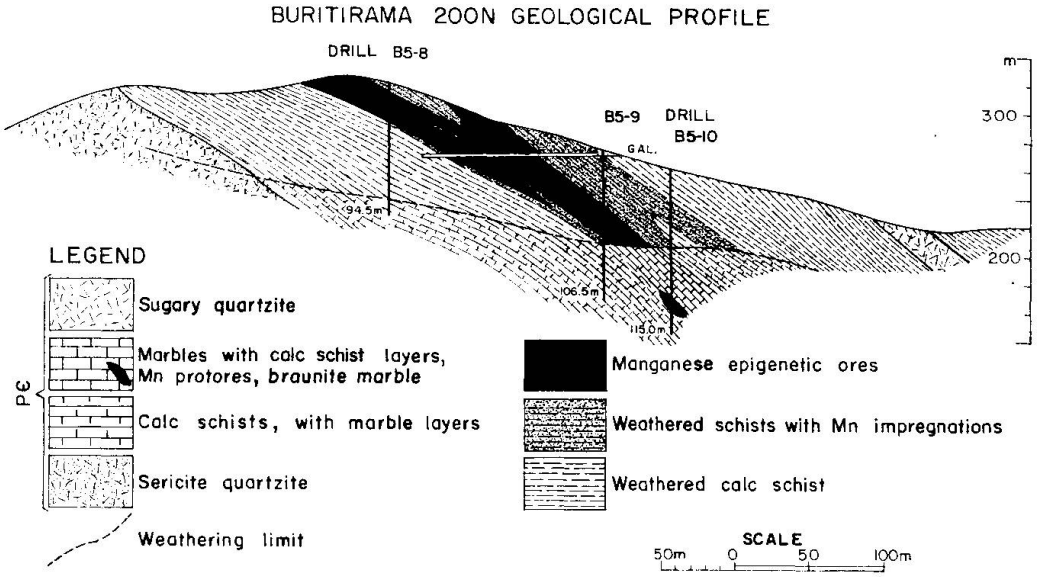

Fig. 3. Geological profile, 200 N of the Buritirama, B-5 orebody after ANDERSON, DYER and TORRES (1974).

manganese oxide and clay minerals that constitutes the bulk of the crude ore (32–46% Mn) until the lowest weathering level is attained at about 60–80 m.

Enveloping the lensoid concentrations of manganese ores and sometimes interlayered with them are zones of weathered schists impregnated with manganese oxides and hydroxides (Fig. 3).

The authigenic manganese minerals of the supergene ore include: cryptomelane, lithiophorite, nsutite, and buserite-like minerals or amorphous MnO_2. Braunite is also present as relicts in the weathered protores. The main gangue minerals are: mica, chlorite, dickite, goethite and (weathered) spessartite.

Wall rocks

The manganese protores are enclosed in a thick banded series of calc – mica schists and calc-silicate marbles interbedded with biotite schists (Fig. 4) (ANDERSON et al., 1974). The most common mineral assemblages are: diopsidic pyroxene + phlogopite + calcite + dolomite, diopside + phlogopite + garnet, tremolite + phlogopite + calcite + dolomite, diopside + phlogopite + K-spar + calcite + dolomite, diopside + quartz, diopside + tremolite + calcite + dolomite + quartz, biotite + garnet + quartz + K-spar + andalusite. Sphene, apatite and tourmaline are common accessories, along veins tremolite forms after diopside and is associated with epidote.

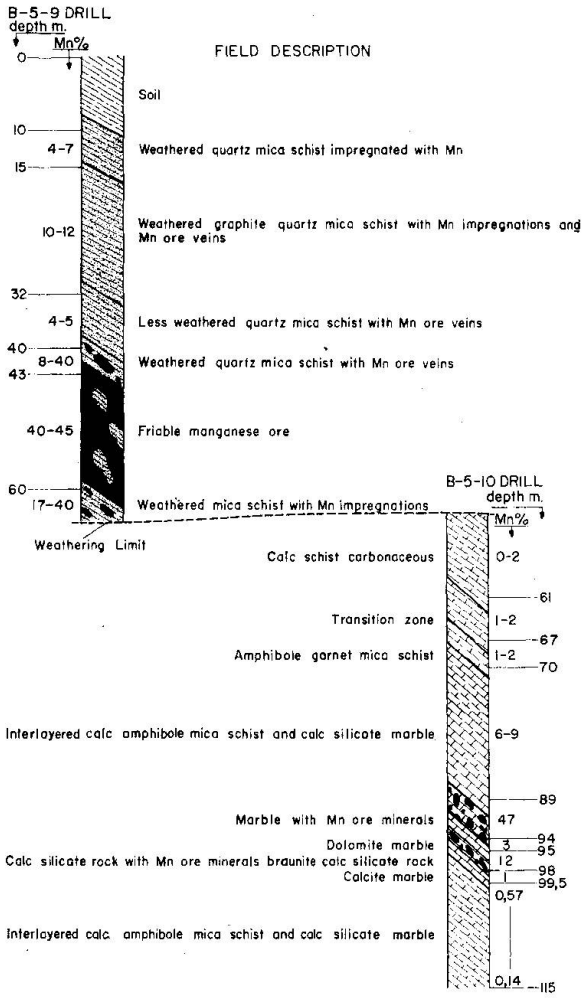

Fig. 4. Schematic lithologic profile of the weathered zone of the B-5-9 diamond drill hole and of the fresh rocks of the B-5-10 diamond drill hole. These drills are located on the Fig. 2 and represented in less detail in Fig. 3. Constructed on the basis description of geologists of Cia Meridional de Mineração and controlled by petrographic and mineralogical studies.

Manganese protores

The protores can be followed through a thickness of 25–30 m and are made up of manganesiferous calc-silicate marbles and manganese-rich calc-silicate schists interlayered with less manganesiferous marbles and schists. Vertical

and horizontal changes in the original sedimentary conditions make it difficult to correlate different drill data.

a) Calc-silicate marble

Poikiloblastic manganese clinopyroxene, Mn-calcite and manganese phlogopite are the main constituents of a mosaic fabric, K-feldspar becoming a major constituent in a few samples. Manganese amphibole may replace clinopyroxene in patches and along veins. Chlorite veinlets can be found cutting the rock.

b) Calc-silicate schist

Manganese phlogopite (manganophyllite), manganese clinopyroxene (johannsenite), spessartite and manganese carbonate are the main constituents. Additional K-feldspar, pyrrhotite and barite may also occur as well as chlorite formed to the expense of manganophyllite.

c) Pyroxmangite calc-silicate marble

These protores are composed of a mosaic intergrowth of manganese-rich carbonate (rhodochrosite), equant spessartite, and large xenoblastic pyroxmangite showing lamellar twinning. Secondary manganese serpentine occurs in narrow veins.

d) Alabandite-tephroite-rhodochrosite marble

Large (2–3 mm) poikiloblastic tephroite crystals are seen beside Ca-rich rhodochrosite, sphalerite, alabandite and spessartite. Accessory pyroxmangite and hausmannite are also present.

e) Braunite-manganoan calcite marble

Masses of braunite are intimately intergrown with manganoan calcite, manganophyllite, K-feldspar and manganoan clinopyroxene. Massive rhodonite and quartz occur in veins. Some secondary formation of a manganese-rich amphibole (dannemorite) after rhodonite is common. During this alteration, fine grained carbonate may be formed.

Mineralogy of the manganese protores

These minerals were normally identified by the usual X-ray and optical means. The chemical compositions of the mineral phases were determined with an ARL electron microprobe type SEMQ, equiped with 6 spectrometers (4 scanners and 2 fixed channels for Si and Al respectively). The following technical parameters were used: 15 KV

acceleration voltage, a sample current of 50 nA for silicates and 10 to 20 nA for carbonates. A fixed beam size of 0.5 micron was applied for silicates, whereas for carbonates the beam was varied between 1 and 20 microns depending on their stability. On each grain up to 10 points were analysed and averaged. Care was taken to analyse assemblages of 2 or more minerals in contact with each other. For the silicate analysis natural silicates and oxides and for the carbonate analysis natural carbonates were used as standard material. For the minor elements at least 10 000 counts were accumulated providing a standard deviation (1 σ) better than 1.0%. The data were on-line corrected for background, deadtime and instrumental drift with a PDP-11/05 computer. Correction procedures for X-ray absorption, X-ray fluorescence and atomic number effects were based on a modified MAGIC IV program fitting the CDC 6500 computer system at the ETH-Zürich.

Carbonates

Carbonates consist almost entirely of $MnCO_3$, $CaCO_3$ and $MgCO_3$. Small amounts (less than 1 mol %) of $FeCO_3$ were also found. No other component could be detected. As seen from the analyses in Table 1 and Fig. 5, the Ca/Mn ratio varies over a wide range, although within one sample the composition

Table 1. Microprobe analysis of carbonates from Mn protores of Buritirama

	Weight %				Mol % end members			
	$MnCO_3$	$CaCO_3$	$MgCO_3$	$FeCO_3$	$MnCO_3$	$CaCO_3$	$MgCO_3$	$FeCO_3$
B-4-14 – 80.8 I	64.2	26.3	7.8	0.7	60.7	28.6	10.1	0.6
B-4-14 – 80.8 II	64.4	25.7	7.5	0.7	61.5	28.1	9.8	0.6
B-4-14 – 80.8 III	71.9	16.9	8.3	0.7	69.6	18.7	11.0	0.6
B-5-10 – 80.2 I	19.1	77.2	2.6	0.2	17.1	77.5	3.2	0.2
B-5-10 – 80.2 II	19.8	73.3	3.1	0.2	18.3	79.7	3.9	0.2
B-5-10 – 80.2 III	16.3	82.8	1.3	n.d.	14.4	84.1	1.5	–
B-5-10 – 92.0 I	20.8	78.3	1.9	n.d.	18.3	79.2	2.3	–
B-5-10 – 92.0 II	20.1	82.1	1.1	n.d.	17.3	81.4	1.3	–
B-5-10 – 97.8 II	11.7	90.3	0.4	n.d.	10.1	89.4	0.5	–
B-5-14 – 67.1 I	50.4	38.9	8.3	0.7	47.1	41.7	10.6	0.6
B-5-14 – 67.1 II	51.5	38.9	8.0	0.7	47.8	41.5	10.1	0.6
B-5-14 – 69.9 I	45.2	47.5	5.8	0.7	41.8	50.3	7.3	0.6
B-5-14 – 69.9 II	44.1	47.5	5.7	0.7	41.2	51.0	7.2	0.6
B-5-14 – 72.0 I	52.4	37.4	9.2	0.7	48.3	39.6	11.6	0.6
B-5-14 – 72.0 II	51.1	36.3	9.0	0.6	48.4	39.5	11.6	0.6
B-5-14 – 72.0 III	52.0	35.7	9.0	0.6	49.1	38.7	11.6	0.6
B-5-14 – 72.0 IV	52.1	36.5	9.1	0.6	48.7	39.2	11.6	0.6
B-5-14 – 78.8 I	50.2	38.8	8.7	0.7	46.8	41.5	11.0	0.6
B-5-14 – 78.8 II	49.1	40.5	8.6	0.7	45.5	43.0	10.8	0.6
B-5-14 – 78.8 III	49.0	40.7	8.7	0.7	45.2	43.2	11.0	0.6
B-5-14 – 78.8 IV	51.0	37.8	8.7	0.7	47.7	40.6	11.1	0.6
B-5-22 – 64.6 I	39.8	53.3	6.6	0.6	36.0	55.3	8.1	0.5
B-5-22 – 64.6 II	38.8	53.4	6.5	0.6	35.4	56.0	8.1	0.5
B-5-22 – 64.6 III	38.0	53.8	6.8	0.6	35.3	56.0	8.5	0.5
B-5-22 – 64.6 IV	39.0	53.0	6.5	0.6	35.7	55.6	8.1	0.6
B-5-22 – 65.8 I	40.9	50.5	7.1	0.7	37.4	53.1	8.9	0.6
B-5-22 – 65.8 II	41.2	51.2	6.7	0.7	37.5	53.5	8.3	0.6
B-5-22 – 65.8 III	41.0	49.0	7.6	0.7	37.8	51.9	9.6	0.7
B-5-22 – 65.8 IV	38.9	53.1	6.5	0.7	35.5	55.7	8.1	0.7

(First two numbers refer to borehole, third number to depth in meters and roman number to spot on thin section. n.d. = not detected.)

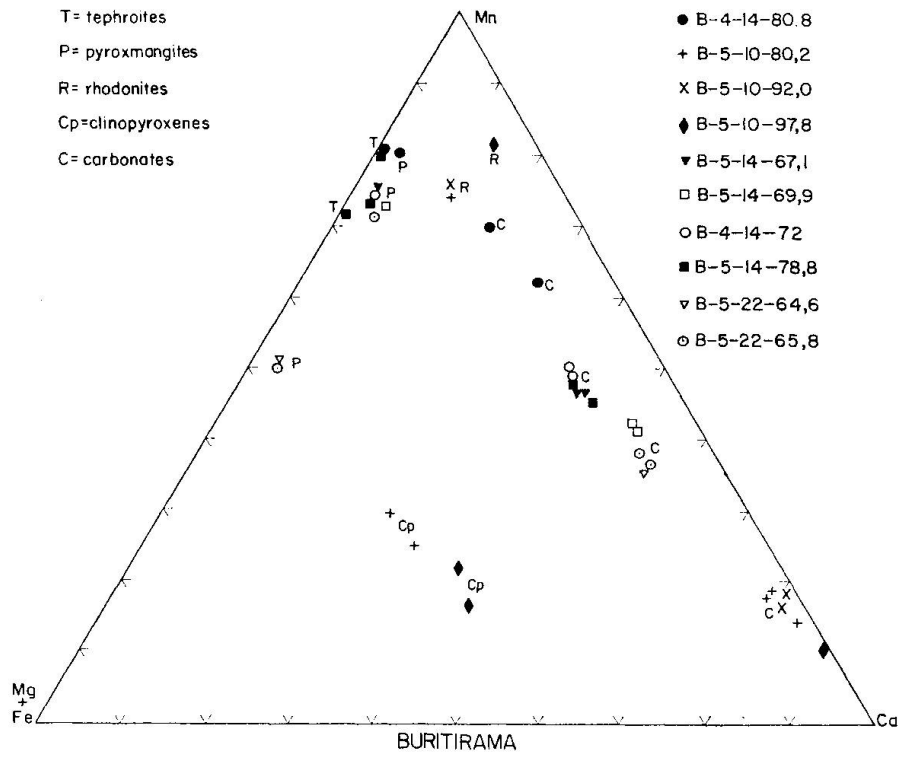

Fig. 5. (Mn)-(Ca)-(Mg+Fe) mol per cent plot of carbonates, rhodonites pyroxmangites, clinopyroxenes and tephroites of manganese protores samples from Buritirama, analyzed by microprobe. The different coexisting phases are plotted with the same graphical symbols.

varies little. The amount of Mg is positively correlated with the Mn/Ca-ratio. Comparing the results with the experimental data of GOLDSMITH and GRAF (1957) in the system $MnCO_3$-$CaCO_3$-$MgCO_3$, most analyses fall within the region of complete miscibility that even at temperatures as low as 500° C extends from $CaCO_3$ toward $Ca_{0.42}Mn_{0.58}CO_3$. Carbonates of one sample have the compositions: $Ca_{0.19}Mn_{0.70}Mg_{0.11}CO_3$ and $Ca_{0.29}Mn_{0.61}Mg_{0.10}CO_3$. At 500° C these would fall within the 2 phase immiscibility field, but at temperatures slightly above 550° C they would lie outside.

Pyroxenoids

Three types of pyroxenoids are common: pyroxmangite, rhodonite and a manganese rich clinopyroxene.

The content of $CaSiO_3$ in the pyroxmangites show little variation (3–4.5 mol %), but the $MgSiO_3$, $FeSiO_3$ and $MnSiO_3$ contents vary strongly as can be seen from the analyses in Table 2 (Fig. 5). With the present data, no correlations between the composition and the optical properties are evident.

Pyroxmangite is the more frequent pyroxenoid and coexists with the manganese richer carbonates (Fig. 5).

Rhodonite occurs in veins and also as a rock-forming mineral coexisting

with the calcium richer carbonates. The $CaSiO_3$ content in the rhodonites varies from 9–11 mol %, and the $MgSiO_3 + FeSiO_3$ content does not exceed 15 mol % (Table 2, Fig. 5). Fig. 5 also shows that rhodonite coexists with a Mn-rich clinopyroxene. No valid correlation between the chemical composition and optical properties is evident with the present data. The manganese-rich clinopyroxene occurs associated with rhodonite and calcium richer carbonates of the calcite-kutnahorite series. Its Fe + Mg content is rather constant, but the Mn/Ca ratios varies appreciably (Table 3). The X-ray pattern can hardly be distinguished from that of johannsenite.

Table 2. Microprobe analysis of pyroxenoids from Mn protores of Buritirama

	Weight %					Numbers of ions on the basis of 3 oxygens				
	SiO_2	MnO	CaO	MgO	FeO	Si	Mn	Ca	Mg	Fe
Pyroxmangites										
B-4-14 – 80.8 III	47.7	44.5	1.09	5.73	0.95	1.00	0.79	0.03	0.18	0.02
B-5-14 – 67.1 I	49.8	42.6	1.45	6.31	1.46	1.01	0.73	0.03	0.19	0.02
B-5-14 – 67.1 II	48.2	42.7	1.47	6.49	1.34	1.00	0.75	0.03	0.20	0.02
B-5-14 – 69.9 I	48.9	41.8	2.09	6.23	1.86	1.00	0.73	0.05	0.19	0.03
B-5-14 – 72.0 I	48.5	42.4	1.43	6.88	1.34	1.00	0.74	0.03	0.21	0.02
B-5-14 – 72.0 II	48.2	42.4	1.43	7.13	1.30	0.99	0.74	0.03	0.22	0.03
B-5-14 – 72.0 IV	48.7	42.5	1.39	6.55	1.30	1.00	0.73	0.05	0.20	0.02
B-5-14 – 78.8 II	48.2	42.9	1.57	6.75	1.28	0.99	0.75	0.03	0.21	0.03
B-5-14 – 78.8 III	48.1	42.1	1.41	7.31	1.29	0.99	0.74	0.03	0.23	0.02
B-5-14 – 78.8 IV	47.8	42.2	1.38	7.36	1.26	0.99	0.74	0.03	0.23	0.02
B-5-22 – 64.6 II	52.6	30.2	1.70	14.98	1.62	1.01	0.49	0.03	0.43	0.03
B-5-22 – 64.6 IV	52.7	30.4	1.61	14.90	1.65	1.01	0.49	0.03	0.42	0.03
B-5-22 – 65.8 I	52.3	30.6	1.46	14.97	1.77	1.01	0.50	0.03	0.43	0.03
B-5-22 – 65.8 II	50.1	41.2	1.72	6.82	1.84	1.01	0.70	0.04	0.21	0.03
B-5-22 – 65.8 IV	50.2	41.4	1.94	6.44	1.94	1.01	0.71	0.04	0.19	0.02
Rhodonites										
B-5-10 – 80.2 II	48.9	41.6	5.01	4.50	0.62	1.01	0.73	0.11	0.14	0.01
B-5-10 – 92.0 I	46.8	43.0	4.83	4.15	0.05	0.99	0.77	0.11	0.13	0.01
B-5-10 – 97.8 IV	48.5	45.0	6.00	1.61	0.15	1.01	0.79	0.13	0.05	0.00

Table 3. Microprobe analysis of clinopyroxenes from Mn protores of Buritirama

	Weight %						
	SiO_2	MnO	CaO	MgO	FeO	Al_2O_3	Na_2O
B-5-10 – 80.2 I	53.0	14.9	15.6	14.9	1.02	0.23	0.24
B-5-10 – 80.2 II	53.3	18.3	12.4	14.6	1.33	0.12	n.d.
B-5-10 – 97.8 II	53.7	13.2	19.4	13.7	0.17	0.10	n.d.
B-5-10 – 97.8 IV	54.1	11.4	20.4	14.4	0.12	0.07	n.d.
	Numbers of ions on the basis of 3 oxygens						
	Si	Mn	Ca	Mg	Fe	Al	Na
B-5-10 – 80.2 I	1.00	0.24	0.32	0.42	0.02	0.01	0.01
B-5-10 – 80.2 II	1.01	0.29	0.25	0.41	0.02	–	–
B-5-10 – 97.8 II	1.01	0.21	0.39	0.38	–	–	–
B-5-10 – 97.8 IV	1.01	0.18	0.40	0.40	–	–	–

Tephroite

Tephroite is a mineral as common in the Mn marble of Buritirama as is in other Brazilian carbonatic protores (Serra do Navio and Lafayette). In Buritirama this mineral commonly grows as oriented poikilitic crystals of up to 3 mm length.

5 measurements from 2 samples gave: $2V_x$ 62–69°.

In addition to Mn_2SiO_4, Buritirama tephroite contains about 15 mol % of Mg_2SiO_4 (forsterite), and trifling amount of Fe_2SiO_4 (fayalite) and Ca_2SiO_4 (larnite) (Fig. 5). The forsterite contents manifests itself in a notable displacement of the X-ray reflections towards lower angles as compared with those of pure Mn_2SiO_4.

Table 4. Microprobe analysis of tephroites from Mn protores of Buritirama

	Weight %						Number of ions on the basis of 4 oxygens					
	SiO_2	MnO	CaO	MgO	FeO	ZnO	Si	Mn	Ca	Mg	Fe	Zn
B-4-14 – 80.8 I	30.7	59.4	0.06	6.24	3.49	n.d.	0.99	1.61	–	0.30	0.09	–
B-4-14 – 80.8 II	30.9	59.4	0.08	6.83	3.42	n.d.	0.99	1.60	–	0.31	0.09	–
B-4-14 – 80.8 III	31.6	59.0	0.07	6.73	3.55	n.d.	1.00	1.60	–	0.31	0.09	–
B-5-14 – 78.8 I	31.6	54.2	0.06	9.98	4.46	0.16	0.99	1.42	–	0.46	0.12	–
B-5-14 – 78.8 II	31.0	54.4	0.07	9.70	4.72	0.12	0.98	1.42	–	0.45	0.12	–
B-5-14 – 78.8 III	31.3	54.0	0.07	9.98	4.63	0.21	0.98	1.41	–	0.46	0.12	0.01
B-5-14 – 78.8 IV	31.0	53.4	0.06	10.94	4.58	0.22	0.97	1.42	–	0.51	0.12	0.01

Manganese amphibole

The manganese clinoamphibole, which is generally formed in parts of the rocks where the partial pressures of H_2O was high, can be named either a manganese-rich cummingtonite or a magnesium-rich dannemorite. Under the microscope this mineral is colorless, or rarely yellow. It may show polysynthetic twinning and its $2V_x$ is $\sim 85°$. The genesis of this mineral seems to be related to the (hydrothermal?) alteration of pyroxenoids and pyroxenes in veins. A few microprobe data are presented in Table 5.

Table 5. Microprobe analysis of amphiboles from Mn protores of Buritirama

	Weight %							
	SiO_2	Al_2O_3	CaO	MgO	MnO	FeO	TiO_2	Na_2O
B-5-10 – 92.0 II	56.9	0.06	11.19	22.0	5.83	n.d.	n.d.	0.34
B-5-14 – 69.9 I	56.4	0.06	0.85	20.1	18.70	2.41	n.d.	0.05
B-5-22 – 64.6 I	54.4	0.19	0.92	19.5	19.94	2.17	n.d.	0.08
B-5-22 – 64.6 IV	56.4	0.14	0.91	19.4	19.14	2.17	n.d.	n.d.
	Numbers of ions on the basis of 23 (O, OH)							
	Si	Al	Ca	Mg	Mn	Fe	Ti	Na
B-5-10 – 92.0 II	7.99	0.01	1.68	4.60	0.69	–	–	0.09
B-5-14 – 69.9 I	8.03	0.01	0.13	4.25	2.25	0.29	–	0.01
B-5-22 – 64.6 I	7.92	0.03	0.14	4.22	2.46	0.26	–	0.02
B-5-22 – 64.6 IV	7.99	0.02	0.14	4.14	2.30	0.26	–	–

Table 6. Microprobe analysis of spessartite from Mn protores of Buritirama

	Weight %							Numbers of ions on the basis of 12 oxygens						
	SiO_2	Al_2O_3	MnO	CaO	MgO	FeO	TiO_2	Si	Al	Mn	Ca	Mg	Fe	Ti
B-4-14 – 80.8 I	37.0	21.2	40.6	1.06	0.72	1.13	0.07	2.98	2.02	2.77	0.09	0.09	0.08	–
B-4-14 – 80.8 II	36.6	21.3	40.4	1.54	0.75	0.76	0.31	2.96	2.03	2.77	0.13	0.09	0.05	0.02
B-5-10 – 80.2 I	37.4	18.9	34.9	4.66	1.80	3.30	n.d.	3.03	1.81	2.39	0.40	0.22	0.22	–
B-5-10 – 92.0 I	36.9	22.6	34.0	4.96	2.61	0.84	0.40	2.90	2.09	2.26	0.42	0.30	0.05	0.02
B-5-14 – 72.0 I	36.9	21.2	38.2	1.90	1.54	1.11	0.20	2.98	2.01	2.61	0.16	0.18	0.07	0.01
B-5-14 – 72.0 II	37.5	21.2	37.7	2.23	1.34	0.89	0.53	3.01	2.00	2.56	0.19	0.16	0.06	0.03
B-5-14 – 72.0 IV	37.8	21.1	38.6	1.66	1.19	1.13	n.d.	3.02	1.99	2.61	0.14	0.14	0.08	–
B-5-14 – 78.8 I	37.5	21.3	39.3	2.00	1.14	1.03	0.28	2.98	2.00	2.63	0.17	0.13	0.07	0.03
B-5-22 – 64.6 I	37.7	21.2	38.2	2.16	1.26	1.03	0.33	3.01	1.99	2.58	0.19	0.15	0.07	0.02
B-5-22 – 64.6 II	37.7	21.2	38.3	2.18	1.18	1.02	0.21	3.00	2.00	2.60	0.19	0.14	0.07	0.01
B-5-22 – 64.6 III	37.5	21.2	37.9	2.26	1.23	1.03	n.d.	3.01	2.00	2.57	0.19	0.15	0.07	–
B-5-22 – 65.8 I	37.3	21.2	38.7	2.12	1.06	1.19	n.d.	2.99	2.00	2.62	0.18	0.13	0.08	–
B-5-22 – 65.8 V	38.0	21.3	38.3	2.10	1.09	1.25	n.d.	3.02	1.99	2.58	0.18	0.13	0.08	–

Garnets

Garnet compositions are close to the spessartite end member but usually comprise small proportions of grossularite, pyrope, almandine, and andradite (Table 6). Garnet is closely associated with carbonates either as inclusions or as a host to carbonatic pigments. In general coarser garnets are confined to silicate (pyroxenoid) richer parts. The cell parameter for garnets varies from 11.570 to 11.634 Å and the measured refractive indices (1.71–1.79) indicate a spessartitic end member with a tendency of some deviation towards grossularite.

Manganoan phlogopite

Manganoan phlogopite (manganophyllite) is a common hydroxylbearing mineral in most assemblages. The manganese content varies little, but the amounts of iron, although low compared with magnesium, differ. The substitution of Na^+ for K^+ is generally negligeable (Table 7).

Table 7. Microprobe analysis of manganese phlogopites from Buritirama

	Weight %								
	SiO_2	Al_2O_3	CaO	MgO	MnO	FeO	K_2O	Na_2O	TiO_2
B-5-10 – 80.2 I	39.4	13.0	0.05	21.7	3.80	4.41	10.20	0.04	2.08
B-5-10 – 92.0 II	39.1	13.4	n.d.	22.2	7.85	0.29	10.12	0.09	0.69
B-5-10 – 97.8 I	39.2	14.3	n.d.	22.0	6.17	0.33	10.16	0.07	0.55
B-5-14 – 67.1 I	39.2	13.8	n.d.	23.4	4.11	2.00	8.72	0.49	0.52
B-5-14 – 72.0 III	39.1	13.3	n.d.	23.8	3.56	1.74	8.94	0.40	0.84
B-5-22 – 64.6 II	39.3	12.6	0.04	23.5	3.42	2.14	9.19	0.19	1.39
	Numbers of ions on the basis of 22 oxygens								
	Si	Al	Ca	Mg	Mn	Fe	K	Na	Ti
B-5-10 – 80.2 I	5.74	2.22	0.01	4.73	0.47	0.54	1.89	0.01	0.23
B-5-10 – 92.0 II	5.74	2.31	–	4.87	0.98	0.04	1.90	0.03	0.08
B-5-10 – 97.8 I	5.76	2.48	–	4.82	0.77	0.04	1.90	0.02	0.06
B-5-14 – 67.1 I	5.74	2.38	–	5.13	0.51	0.25	1.63	0.14	0.06
B-5-14 – 72.0 III	5.76	2.30	–	5.23	0.44	0.21	1.68	0.11	0.03
B-5-22 – 64.6 II	5.79	2.19	0.01	5.15	0.43	0.26	1.78	0.05	0.13

Ore minerals

Braunite is an abundant mineral in the braunite marble protore. It presents a massive aspect being frequently cut by veins containing: carbonates + manganophyllite + manganese clinoamphibole. Bixbyite is an occasional associate. The braunite's SiO_2 content is nearly constant and supports the ideal formula: $3\,Mn_2O_3 \cdot MnSiO_3$. Substitutions of Fe and Al for Mn^{3+} in the first part of this formula arc quite restricted, as are the substitution of Ca and Mg for Mn^{2+} in the second part of the formula.

Alabandite was found in one sample (B–4–14 drill) where it is associated with accessory pyrrhotite in a rhodochrosite-tephroite-spessartite rock. It occurs as large xenomorphic grains containing some Fe and traces of Mg.

Sphalerite occurs as an accessory. Beside Zn some Fe and Mn were also found. Its microscopic red colour makes it almost indistinguishable from pyrophanite – $MnTiO_3$ – a relatively common protore accessory. Microprobe analyses show some CaO and FeO in the latter mineral. Hausmannite is a rare accessory found in the braunite marble protore. It contains about 5 mol % of Fe_3O_4, besides Mn_3O_4.

Mineral assemblages

The following manganese-bearing mineral assemblages were encountered among the analysed suits.

01) carbonate + pyroxmangite + tephroite
02) tephroite + carbonate + spessartite + pyrophanite
03) tephroite + carbonate + pyroxmangite + spessartite
04) carbonate + tephroite + spessartite + alabandite (+ sphalerite)
05) carbonate + braunite + manganophyllite + manganese amphibole
06) manganese clinopyroxene + carbonate + manganophyllite + spessartite
07) manganese clinopyroxene + rhodonite + carbonate
08) rhodonite + carbonate + spessartite
09) manganese clinopyroxene + rhodonite + carbonate + braunite
10) manganese clinopyroxene + manganese clinoamphibole + manganophyllite + spessartite + carbonate
11) pyroxmangite + manganophyllite + carbonate
12) pyroxmangite + manganese clinoamphibole + carbonate + spessartite
13) pyroxmangite + carbonate + spessartite + manganophyllite
14) carbonate + braunite + hausmannite (+ bixbyite)
15) carbonate + hausmannite
16) rhodonite + carbonate + manganophyllite + K-spar + spessartite ± baryte
17) quartz + rhodonite + carbonate
18) quartz + braunite + rhodonit

Neglecting the small amounts of Fe and assuming CO_2, H_2O and S to be perfectly mobile components, one is left either with the 5 component system Mn-Ca-Mg-Al-Si or, including K (in manganophyllite and K-spar), with a 6 component system. Manganophyllite free assemblages contain mostly 4 phases, which makes the system trivariant.

Fluid inclusions

In addition to chemical and mineralogical data first results from fluid-inclusion research may be interesting for evaluation of P-T data.

In quartz grains coexisting with different manganese minerals several generations of fluid inclusions have been recognized which are mainly bound to small healed fractures. In general earlier generations have very high con-

centrations of CO_2, whereas later ones show low values of X_{CO_2} with three phases (CO_2l, CO_2g, H_2Ol). Latest stages present water solutions of high salinity, even with small solid inclusions.

The earliest inclusions, supposed to have formed during the main metamorphic event, constantly show one or two phases of CO_2. The observed homogenizations, always towards liquid CO_2, indicate hight densities. In the diagram (Fig. 6) two main populations of homogenization temperatures and corresponding densities (LANDOLT-BOERNSTEIN tables, 1960) can be recognized, indicating decompression of the fluid.

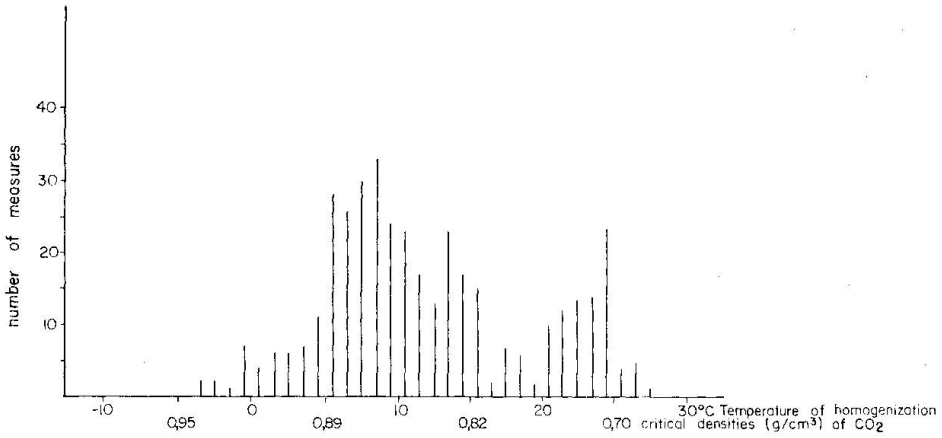

Fig. 6. Critical densities (g/cm³) of CO_2 and temperature of homogenization of 394 fluid inclusions in quartz crystals from Buritirama (B-5-10) braunite marble manganese protore. The quartz occurs in small aggregates associated with different manganese minerals.

The earlier population, with higher densities can be interpreted in two ways: a) as a true population with a main value of homogenization temperature of 8–9° C and a main density of 0.87, or b) only the highest values with homogenization temperatures from −5–0° C and densities of 0.95–0.93 are significant, the other values testifying later stages of decompression. Both interpretations are feasible, and at the moment no preference can be given to one or the other.

The linear extrapolation of P-V-T data for CO_2 (KENNEDY, 1954) from isochores d = 0.95 g/cm³ (maximum values) and d = 0.87 g/cm³ (main value) gives P-T-gradients of 10° C/78.5 bars (33° C/km, maximum value) or 10° C/53 bars (54° C/km, main value). As influences of decompressibility and dilatancy of quartz can be neglected, pressures can be calculated, if temperatures are known.

Physical-chemical conditions during metamorphism

The mineral assemblages in the rocks associated with the manganese-protores indicate a metamorphism in the lower to middle amphibolite facies.

No invariant assemblages that could be used as a precise geothermometer and geobarometer were encountered. From the composition of the Ca-Mn-Carbonates a minimum temperature of 540° C can be deduced. In some rocks the isobaricly invariant assemblage diopside + tremolite + calcite + dolomite + Qz was found, indicating a high X_{CO_2} and temperatures between 500° C and 600° C depending upon the total pressure. These high partial pressures of CO_2 inferred by the mineral assemblages support the assumption that the first generation fluid inclusions with the high CO_2 content formed at the main metamorphic event. The mean density of CO_2 in most inclusions of the first generation (Fig. 6) is 0.87 g/cm². Assuming a temperature of 550 ± 50° C, a total pressure of 3 ± 0.3 Kb results.

For the estimation of the oxygen fugacity during metamorphism the assemblages manganese carbonate-braunite, carbonate-braunite-hausmannite and hausmannite-carbonate are important. In the pure system Mn-Si-C-O (PETERS, VALARELLI and CANDIA, 1974) the second assemblage would be isobaricly invariant, that would fix log f_{O_2} at −10. However, the carbonate is not pure $MnCO_3$, but a solid solution of $CaCO_3$ and $MnCO_3$, meaning an activity of less than 1 for $MnCO_3$ in the equilibrium $6MnCO_3 + O_2 = 2Mn_3O_4 + 6CO_2$ resulting in an even higher f_{O_2} compared with pure $MnCO_3$.

Ore genesis

The manganese ore of Buritirama has a complex history, of which only the latest stages can be evaluated with some confidence.

The latest event is the enrichment of manganese by supergene weathering from Mn-bearing calc-silicate marbles. Although the bulk of the carbonates has a relatively low Mn-content they weather easily, giving an ore rich in highly oxidized manganese oxides and hydroxides. A regional metamorphism in amphibolite facies has determined the mineralogy and texture of the protore. The effects of a later retrograde metamorphism are small. During the strong metamorphic event manganese was enriched in the silicate phases (pyroxenoides, garnets and tephroite) as they formed from the reaction of Ca-Mn-Carbonates with quartz and phyllosilicates. Contemporaneously dolomite reacted with SiO_2 to form diopsidic clinopyroxenes and calcite.

The strong regional metamorphism has obliterated practically all sedimentological evidences of the original deposition. The succesion of quartzites, manganiferous calc-silicate marbles and muscovite quartzites in Buritirama is comparable with the manganiferous limestone dolomite formations as defined by VARENTSOV (1964). Together with the relatively high oxidation state and high Ba-content of the Buritirama protores a succession formed in a shallow platform basin is indicated. The graphite-bearing Mn-rich protores of Amapa

and Lafayette associated with black bitumous pyritiferous shales formed in an enviroment transitional to deeper water. The ore material was probably derived from weathering of the gneisses and amphibolites of the underlying Xingu Complex. An additional volcanic supply cannot be excluded as there is evidence for basic volcanic activity in the Grão Pará Group in the Serra dos Carajás region.

Acknowledgments

The authors thank Dr. Robert C. Dyer and Dr. Warren L. Anderson of "Companhia Meridional de Mineração" who gave the permission to publish this paper and for their cooperation in collecting the samples. The CNPq ("Conselho Nacional de Pesquisas do Braseil") and the FAPESP ("Fundação de Amparo à Pesquisa do Estado de São Paulo"), which furnish the financial assistance for a stay of T. P. at S. Paulo university and of J. V. V. at Bern and Fribourg University, are gratefully acknowledged. Mr. M. Engi is thanked for his comments. The Swiss National Science Foundation supported this project.

References cited

Abrecht, J. and Tj. Peters (1975): Hydrothermal synthesis of Pyroxenoids in the system $MnSiO_3$-$CaSiO_3$ at Pf = 2Kb. Contr. Mineral. Petrol. *50:* 241–246.

Anderson, W. L., R. C. Dyer and D. D. Torres (1974): Ocorrências de manganês na Bacia do Rio de Itacaiunas, Centro-Leste do Estado do Pará. Anais 28° Congr. Bras. Geol. *6:* 149–164.

Beisiegel, W. R., A. L. Bernardelli, N. F. Drummond, A. W. Ruff and J. W. Tremaine (1973): Geologia e recursos minerais da Serra dos Carajás. Rev. Brasil. Geociências *3:* 215–242.

Galeão da Silva, G., M. I. C. Lima, A. L. F. Andrade, R. S. Issler and G. Guimaraes (1974): Geologia das Folhas SB-22 Araguaia e parte da SC-22 Tocantins. Projeto RADAM *4:* 1–143.

Goldsmith, J. R. and D. L. Graf (1957): The system CaO-MnO-CO_2: solid solutions and decomposition relations. Geochim. et Cosmochim. Acta *II:* 310–344.

Gomes, C. B., U. G. Cordani and M. A. S. Basei (1975): Radiometric ages from the Serra dos Carajás Area, Northern, Brazil. Geol. Soc. America Bull. *86:* 939–942.

Kennedy, G. C. (1954): PVT relations in CO_2 at elevated temperatures and pressures. Amer. J. Sci. *252:* 225–241.

Landolt-Boernstein Tables (1960): Eigenschaften der Materie in ihren Aggregatzuständen, v. 2, IIa, Springer-Verlag.

Peters, Tj., J. V. Valarelli and M. A. F. Candia (1974): Petrogenetic grids on the system Mn-Si-C-O-H. Rev. Brasil. Geociencias *4:* 15–26.

Tolbert, G. E., J. W. Tremaine, G. C. Melcher and C. B. Gomes (1971): The recently discovered Serra dos Carajás iron deposits, northern Brazil. Econ. Geology *66:* 985–994.

Varentsov, I. M. (1964): Sedimentary Manganese Ores. Elsevier Publ. Co. Amsterdam.

Manuscript received September 14, 1977.